# Spin Momentum Transfer and Oersted Field Induce a Vortex Nano-Oscillator in Thin Ferromagnetic Film Devices

M. A. Hoefer* and T. J. Silva
*National Institute of Standards and Technology, Boulder, Colorado 80305, USA*
(Dated: May 25, 2019)

A nonlinear model of spin-wave excitation involving a point contact in a thin ferromagnetic film that includes the Oersted magnetic field contribution is presented. We consider the case of an external dc field applied perpendicular to the film plane. The two-dimensional vectorial model reduces to an exact one-dimensional equation of motion. Large-amplitude vortex modes are computed, which represent a fundamental shift in the geometrical understanding of spin transfer nano-oscillators. Odd symmetry forces the magnetization to be pinned in the center of the point contact. Using the spin transfer efficiency as a single fitting parameter, the calculated dependence of frequency on current and contact size is in good agreement with recent experimental data. These vortex states are geometrically very different from previously computed cylindrical modes that exhibit even symmetry when the Oersted field is ignored.

PACS numbers: 75.30.Ds, 75.40.Gb, 75.70.-i, 76.50.+g

Microwave generation due to spin-momentum transfer (SMT) in a thin magnetic multilayer has potential applications in communications and high-density data storage. Established linear and nonlinear theories based on a simplified one-dimensional geometry have neglected contributions from the *two-dimensional* Oersted field intrinsic to all SMT devices [1, 2, 3]. In this study, we develop and analyze an exact *one-dimensional* nonlinear theory of spin-momentum transfer induced magnetodynamics in the presence of an Oersted field.

Thin film, multilayer point contact systems (e.g., Fig. 1 of [1]) have been shown experimentally to generate microwaves caused by steady-state precession of the magnetization in the ferromagnetic Permalloy ($Ni_{80}Fe_{20}$) free layer [4, 5]. A magnetic field $H_0\hat{z}$, large enough to saturate the magnetization, is applied perpendicularly to a thin film multilayer stack. When a dc current $I$ is applied through a point contact of radius $r_*$ into the multilayer $Co_{81}Fe_{19}/Cu/Ni_{80}Fe_{20}$, the conduction electrons' spins induce a torque on the magnetization in the free layer due to conservation of angular momentum [6, 7]. This torque opposes the damping of the free layer and produces dynamics. Ampère's law implies that the dc current $I$ also induces a magnetic field: The Ampèrian or Oersted field $\vec{H}_J$. This field, oriented in the azimuthal direction, is two-dimensional and of comparable magnitude to the other fields in the problem. This fundamental contribution to magnetization dynamics has been considered numerically in the case of in-plane applied fields only [8]; this is the first study to consider the Oersted field for a perpendicular applied field.

Understanding the SMT effect in point contacts with a perpendicular field geometry is of great interest as it tends to yield narrower line widths and higher output powers [4, 9] when compared to other SMT geometries, such as in-plane fields [10]. In addition, this highly symmetric configuration is most amenable to analytical study. Insights derived from this simpler geometry may aid in solving the more advanced problem of oblique angled fields.

In this Letter, we derive a new, exact, one-dimensional model of spin wave excitation in the presence of an Oersted field. An analytical expression for the Oersted field in point contact devices is presented. In the presence of this field, solutions to the vectorial model are shown to be of vortex type, where the magnetization is pinned at the center of the point contact, and exhibit odd symmetry. Coherently precessing spiral modes are found via numerical integration. The calculated frequencies agree with recent experimental observations [5] and show the importance of the Oersted field in modeling SMT-induced magnetization dynamics.

Zero temperature dynamics of the free layer magnetization $\vec{M}$ can be described by the vectorial equation [1]

$$\frac{\partial \vec{M}}{\partial t} = \underbrace{-|\gamma|\,\mu_0 \vec{M}\times\vec{H}_{\rm eff}}_{\text{precession}} \underbrace{-\frac{2}{M_s^2 T_2}\vec{M}\times(\vec{M}\times\vec{H}_{\rm eff})}_{\text{Landau-Lifshitz damping}} + \underbrace{\beta(\vec{x})\vec{M}\times(\vec{M}\times\hat{m}_{\rm F})}_{\text{Slonczewski SMT torque}}, \quad (1)$$

where the precessional and damping terms are determined by the effective magnetic field

$$\vec{H}_{\rm eff} = \frac{2\pi D}{|\gamma|\,\mu_0 M_s h}\nabla^2\vec{M} + H_0\hat{z} - M_z\hat{z} + \vec{H}_J. \quad (2)$$

This field consists of respectively the exchange field, the perpendicularly applied field, the demagnetizing field due to axial dipole coupling, and the Oersted field $\vec{H}_J$ satisfying the equations $\nabla\times\vec{H}_J = \vec{J}(\vec{x})$, $\nabla\cdot\vec{H}_J = 0$, where $\vec{J}$ is the current density.

Crystalline anisotropy is assumed to be negligible. Since the free layer film thickness $\delta$ is much smaller than

the transverse length scale set by the diameter of the point contact, $\delta = 4.5$ nm $\ll 2r_*$, where $2r_*$ ranges from 35 nm to 280 nm; in the experiments considered here, we neglect in-plane dipole coupling and assume $\frac{\partial \vec{M}}{\partial z} \approx 0$ (see [11] for an asymptotic argument justifying this simplification). The Landau-Lifshitz form of damping is a commonly used phenomenological term that drives the magnetization to align with the total field. The Slonczewski spin momentum torque (SMT) term is derived in [6] and assumes a large, bulk ferromagnetic layer with fixed magnetization direction $\hat{m}_{\rm F} = \hat{z}$. Relevant parameters are the gyromagnetic ratio ($\gamma$), Planck's constant ($h$), the free space permeability ($\mu_0$), the exchange parameter ($D$), the saturation magnetization ($M_s$), and the transverse relaxation time ($T_2$); $\beta(\vec{x})$ is the SMT driving term modeled by a step function [1]. Since the patterned multilayer mesa used in experiments is roughly two orders of magnitude wider than the point contact [5], we assume that the magnetic free layer has infinite extent in the $xy$ plane; hence $0 \le r < \infty$.

The current density $J(\vec{x})$ is modeled as

$$\vec{J}(r,z) = \hat{r}\frac{I}{2\pi D_p r_*}F(r)[H(z-A/2)H(A/2+D_p-z) - H(z+A/2)H(-A/2-D_p-z)] - \hat{z}\frac{I}{\pi r_*^2}H(r)H(r_*-r)H(z+A/2)H(A/2-z),$$
$$F(r) = \begin{cases} r/r_* & 0<r<r_* \\ r_*/r & r_*<r \end{cases}, \quad H(x) = \begin{cases} 0 & x<0 \\ 1 & x>0 \end{cases}. \tag{3}$$

This current density models the situation depicted in Fig. 1. Two parallel conductor plates of thickness $D_p$ are assumed to have infinite extent because the experimental leads are more than an order of magnitude larger than the point contacts. These plates are connected by a wire of radius $r_*$. Current flows into the wire from the upper plate, through the free layer via a cylinder modeling the point contact, and out of the wire into the lower plate. The current flow in the plates is assumed to be in the radial direction $\hat{r}$ only. The distance between the plates is $A$. The coefficient of $\hat{r}$ in (3) models the magnitude of the current density in the plates, assumed uniform in the $z$ direction. Outside of the region, where the wire connects to the plates ($r > r_*$), the current density falls off proportional to $1/r$, whereas inside the region ($r < r_*$), the current is proportional to $r$. The current is assumed to flow uniformly down the wire modeled by the coefficient of $\hat{z}$ in (3). This model of current flow conserves the flux of current from the plates to the wire. In this coordinate system, the location of the magnetic free layer $z_*$, where the magnetization dynamics occur, is shown in Fig. 1. We are interested in the value of the Oersted field $\vec{H}_J$, due to the current density (3) in the plane $z = z_*$ of the free layer magnetization.

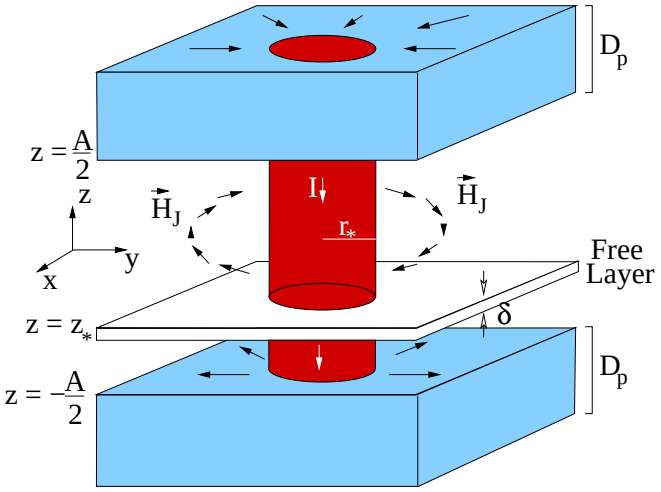


FIG. 1: (Color online). Current density schematic for point contact experiments. Two conductive plates of finite thickness carry current into and away from a point contact device connecting a wire to a ferromagnetic free layer. Ampère's law states that a magnetic field is generated whenever there is a current. By the spin momentum transfer effect, the current also imparts a torque to the magnetization in the free layer. The fixed, non-magnetic, insulating, and capping layers have been omitted from this diagram.

Using a vector potential representation along with Fourier and Hankel transforms, we solve for the Oersted field [12]:

$$\vec{H}_J(r,\phi) = -\hat{\phi}\frac{I}{\pi r_*}\{\underbrace{I_{w\infty}(\frac{r}{r_*})}_{\text{infinite wire}} - \underbrace{I_{wa}(\frac{r}{r_*})}_{\text{finite wire correction}} + \underbrace{\frac{r_*}{D_p}[I_{p1}(\frac{r}{r_*}) + I_{p2}(\frac{r}{r_*})]}_{\text{conductive plates}}\}. \tag{4}$$

The integrals in (4) are

$$I_{w\infty}(\rho) = \begin{cases} \rho/2 & 0<\rho<1 \\ 1/2\rho & 1<\rho \end{cases}, \tag{5}$$

$$I_{wa}(\rho) = \int_0^\infty e^{-qa/2}\cosh(q\frac{z_*}{r_*})J_1(q)J_1(q\rho)\frac{1}{q}\,\mathrm{d}q, \tag{6}$$

$$I_{p1}(\rho) = \int_0^\infty e^{-qa/2}(1-e^{-qd})\cosh(q\frac{z_*}{r_*})J_0(q)J_1(q\rho)\frac{1}{q}\,\mathrm{d}q, \tag{7}$$

$$I_{p2}(\rho) = \int_0^\infty e^{-qa/2}(1-e^{-qd})\cosh(q\frac{z_*}{r_*})J_2(q)J_1(q\rho)\frac{1}{q}\,\mathrm{d}q, \tag{8}$$

where $a = A/r_*$, $d = D_p/r_*$ are the normalized wire length and plate thickness, respectively, and $J_n$ are the $n$th-order Bessel functions of the first kind. Note that (4), with $I_{wa} = I_{p1} = I_{p2} \equiv 0$, is the result for the magnetic field due to an infinitely long wire of radius $r_*$ with no

conductive plates. The magnitude of the Oersted field $|\vec{H}_J(r)|$ in (4) depends only on $r$.

By numerically evaluating the integrals (6-8), we show $|\vec{H}_J(r)|$ for two contact sizes and currents in Fig. 2. The fields due to an infinitely long wire with no conductive plates are also shown in Fig. 2 as dashed curves. For the smaller contact ($r_*/D_p$ small), equation (4) and the result for an infinite wire agree very well near the point contact, but this is not the case for the larger contact size where $r_*/D_p$ is large.

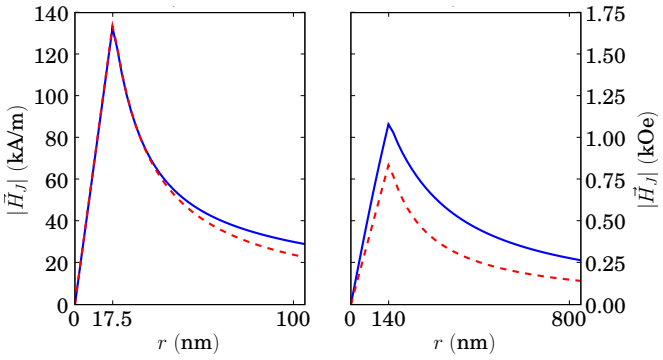


FIG. 2: (Color online). The magnitude of the Oersted magnetic field (4) (solid) and the Oersted field due to an infinitely long wire with no conductive plates (dashed). The left figure depicts the fields for a small contact ($r_* = 17.5$ nm, $I = 15$ mA) showing good agreement between eq. (4) and the infinite wire case near the point contact. In the right figure ($r_* = 140$ nm, $I = 60$ mA), as $r_*/D_p$ increases, the finite result deviates significantly from the infinite wire result because the contribution from the conductive plates becomes important.

Equation (1) without the Oersted field contribution was studied in [1] where it was shown that a one-dimensional coherently oscillating mode solution exists with even symmetry with respect to inversion about $r = 0$. The Oersted field (4) depends on $r$ and $\phi$, forcing equations (1) and (2) to be two-dimensional. We now derive an exact one-dimensional equation by separation of variables as follows:

$$\vec{M}(r,\phi,t) = R(\phi)\vec{M}'(r,t), \tag{9}$$

where $R(\phi)$ is the rotation matrix

$$R(\phi) = \begin{bmatrix} \cos(\phi) & -\sin(\phi) & 0 \\ \sin(\phi) & \cos(\phi) & 0 \\ 0 & 0 & 1 \end{bmatrix}. \tag{10}$$

Inserting (9) into (1) and using the invariance of the cross product with respect to rotations, $R(\phi)(\vec{u}\times\vec{v}) = [R(\phi)\vec{u}]\times[R(\phi)\vec{v}]$, we find that the rotated magnetization vector $\vec{M}'$ satisfies the same dynamical equation (1) as $\vec{M}$ except that the effective field $\vec{H}'_{\rm eff}$ now has no angular $\phi$ dependence

$$\vec{H}'_{\rm eff} = R(-\phi)\vec{H}_{\rm eff} = (H_0 - M'_z)\hat{z} - |\vec{H}_J(r)|\hat{y} + \frac{2\pi D}{|\gamma|\,\mu_0 M_s h}[(\frac{\partial^2}{\partial r^2} + \frac{1}{r}\frac{\partial}{\partial r})\vec{M}' - \frac{1}{r^2}\vec{M}'_\perp], \tag{11}$$

where $\vec{M}'_\perp \equiv (M'_x, M'_y, 0)$ represents the transverse component of the magnetization. Note that we used the identity $R(-\phi)\hat{\phi} = \hat{y}$ to obtain the $\hat{y}$ term in (11). The last term in (11) forces the transverse component to be zero at the origin; hence the magnetization is pinned at the center of the point contact. For zero current, the equilibrium state is $M_s\hat{z}$. Therefore we assume that the magnetization is pinned upward at the center of the point contact, $\vec{M}'(0,t) = M_s\hat{z}$.

In addition to pinning the magnetization, the form of the solution (9) forces the transverse component of the magnetization $\vec{M}_\perp$ to have odd symmetry: $\vec{M}_\perp(r,\phi+\pi,t) = -\vec{M}_\perp(r,\phi,t)$. Thus *any* nonzero Oersted field contribution forces the magnetization into a vortex or spiral-like state. Slonczewski's study of (1) in the small amplitude regime showed the existence of cylindrical oscillating modes with even symmetry [2]. The Oersted field causes a fundamental change in the geometrical structure of the excitations.

We have computed coherently precessing nonlinear modes for equation (1) with the effective field (11). Using the projection method discussed in [13], we evolve a localized initial condition in time with the SMT term set to zero over a large domain ($0 \le r \le 100r_*$) until it relaxes to its equilibrium state. This state is then used as an initial condition for the full model equations, evolved over the same domain, until a coherently precessing mode forms (approximately 2 ns). The frequency of oscillation is numerically recovered by averaging the calculated oscillatory period in the time domain of each component of the magnetization at $r = r_*$. For all calculated frequencies, critical currents, and mode structures, we used a spatial discretization in radius of $r_*/40$. We find that the calculated frequencies and critical currents have errors of less than 1 % when compared with finer discretizations. For a grid spacing of $r_*/7$, the frequencies and critical currents exhibit errors of approximately 10 %. The numerical scheme with grid spacings coarser than $r_*/7$ exhibits unstable behavior.

An example vortex mode is shown in Fig. 3. Since the magnetization amplitudes decay slowly in space to their equilibrium values, these vortices are weakly localized radiating radial spin waves.

Using our one-dimensional model, we can fit recent experimental data [5] extremely well. The authors in [5] studied the contact size dependence of the frequency versus current relationship. The radii of the devices range from 17.5 nm to 140 nm. The nominal parameter values are $D = 6.41\cdot10^{-40}$ J·m$^2$, $M_s = 600$ kA/m, $\delta = 4.5$ nm, $\gamma = 1.85\cdot10^{11}$ Hz/T, damping constant $\alpha = 2/\gamma\mu_0 M_s T_2 =$

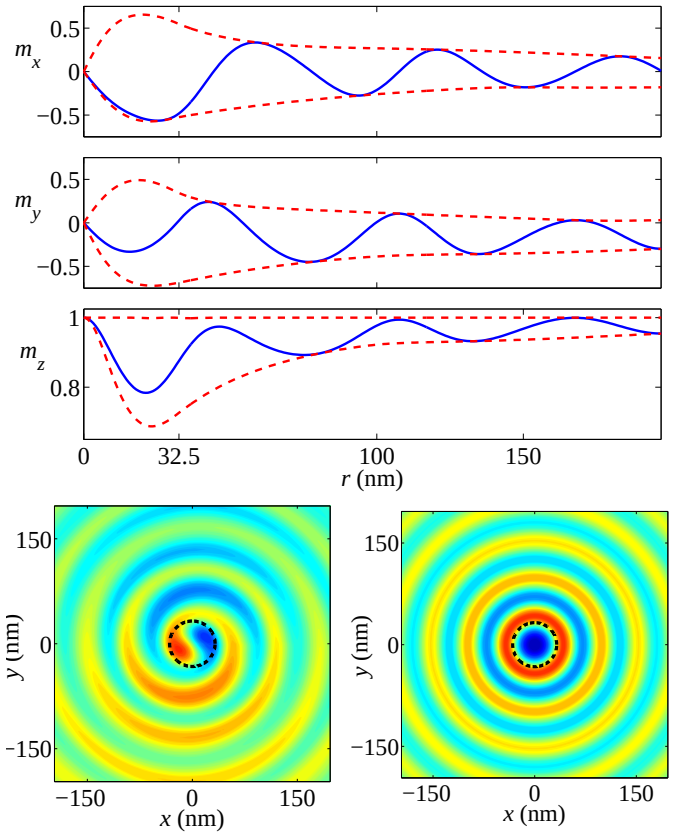


FIG. 3: (Color). Top: Spatial distribution of a numerically calculated coherently precessing vortex mode with frequency 17.1 GHz at $\phi = 0$ at a specific time (solid curves). The dashed curves are the envelopes corresponding to the maxima and minima of the mode as it varies in time. The magnetization is normalized to saturation $m_x = M_x/M_s$. Parameter values include $I = 18$ mA and $r_* = 32.5$ nm. A constant spin torque efficiency of $\varepsilon = 0.26$ was assumed. Bottom, left: A contour plot of $m_x$, the vortex mode with odd symmetry, where redder areas correspond to larger, positive function values and blue areas correspond to smaller, negative function values. The black dashed circle in the center represents the point contact boundary. The two dimensional spiral shape is apparent. Bottom, right: A contour plot of $m_x$, the radially symmetric mode with even symmetry (frequency 18.9 GHz), when the Oersted field is neglected (see [1]).

0.0112, $H_0 = 1.25M_s$, $D_p = 50$ nm, $A = 116$ nm, and $z_* = -30$ nm. We show that by using only $\epsilon$ as a fitting parameter, the theoretical data quantitatively match the experimental data over a wide range of contact sizes.

Figure 4 depicts the frequency versus current relation for different sized point contact devices. The contact radii for each set of experimental data (circles) [5] are shown in the figure. The solid curves correspond to the frequency vs. current relationships for the oscillating vortex modes determined numerically. The dashed lines correspond to the theoretical results in [1] where the Oersted field was neglected. For the two largest contact sizes, 90 and 140 nm, our theory of oscillating vortices agrees with experiment quantitatively. The middle sizes 32.5, 42.5, and 55 nm agree with experiment qualitatively while the smallest contact at 17.5 nm does not. Our theory predicts a critical current and onset frequency of 22.4 mA and 29.4 GHz respectively for the smallest contact, much larger than experiment. The dash-dotted line is a linear extension of our theory to currents below the critical current. In contrast, the theory of even modes where the Oersted field is neglected agrees qualitatively with experiment for the 32.5 nm contact but otherwise deviates significantly from the experimental data. The only fitting parameter used was the spin transfer efficiency $\varepsilon = 0.19$. Previous dc conductance measurements using mechanical point contacts found $\varepsilon = 0.26$ for Permalloy/Cu multilayers [14].

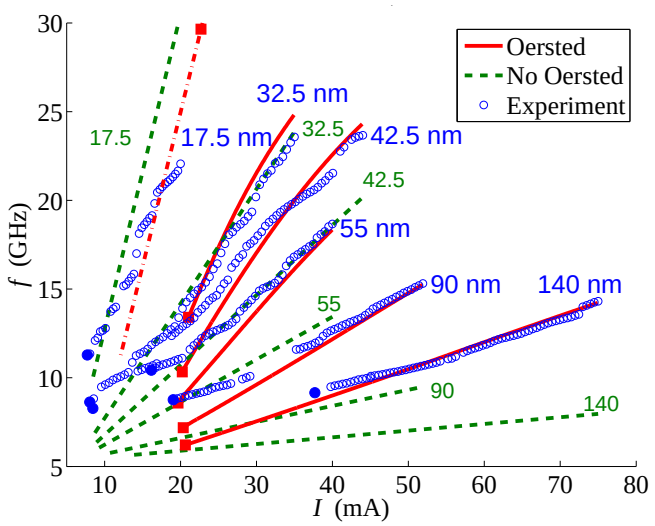


FIG. 4: (Color). Frequency as a function of current for the size dependent point contact experiments in [5] (circles), our theory of oscillating vortex modes with an Oersted field (solid lines), and the theory presented in [1] that ignores the Oersted field (dashed lines with contact size denoted in smaller font). The solid dots correspond to the experimentally observed critical currents whereas the solid squares correspond to the numerically determined critical currents from the onset of oscillations in a vortex mode. The dash-dotted line corresponds to a linear extension of the theoretical vortex mode data below the critical current for the smallest contact with radius $r_* = 17.5$ nm.

The solid squares in Fig. 4 correspond to the numerically determined critical current, the onset current for vortex mode excitation. These values are larger than experiment (solid circles in Fig. 4) for all but the two largest contacts.

Given the odd symmetry of the calculated mode structure, electrical detection of the resultant magnetization dynamics via the giant magnetoresistance effect rests solely upon the time variation of the $z$-component of the magnetization. In particular, $\frac{d}{dt}\int_0^{2\pi}\int_0^{r_*}\vec{M}\cdot\hat{z}\,r\,\mathrm{d}r\,\mathrm{d}\phi \neq 0$, but the odd symmetry of the mode implies that

$\int_0^{2\pi}\int_0^{r_*}\vec{M}\cdot\hat{x}\,r\,\mathrm{d}r\,\mathrm{d}\phi = 0$, in contrast to the case when the Oersted field is ignored [1].

The presence of a vortex core in the mode structure introduces a new mechanism by which instabilities can enter the problem. The exact location of the vortex core is presumably a function of the current distribution in the point contact. While we have modeled the current distribution in an ideal way, centered with respect to the chosen coordinate system, the experimental situation may be more complicated. In particular, the vortex core may tend to be located at nanoscale defects in the polycrystalline structure, such as grain boundaries. Experimentally, hopping of the vortex core between multiple pinning sites may result in frequency instability.

In conclusion, we have shown that by incorporating the two-dimensional Oersted field, coherently oscillating modes in point contact experiments with the perpendicular geometry are weakly localized vortices radiating spin waves. These modes have odd symmetry with the magnetization pinned vertically at the center of the point contact. This model agrees with recent experiments for all but the smallest contact that was measured, and represents a fundamental shift in the geometrical understanding of spin transfer nano-oscillators.

The authors thank W. H. Rippard for suggesting the line of study carried out in this work.

* Electronic address: hoefer@boulder.nist.gov; Contribution of the U.S. Government, not subject to copyright.

[1] M. A. Hoefer, M. J. Ablowitz, B. Ilan, M. R. Pufall, and T. J. Silva, Phys. Rev. Lett. **95**, 267206 (2005).
[2] J. C. Slonczewski, J Magn Magn Mater **195**, L261 (1999).
[3] A. Slavin and V. Tiberkevich, Phys Rev Lett **95**, 237201 (2005).
[4] W. H. Rippard *et al.*, Phys Rev Lett **92**, 027201 (2004).
[5] F. B. Mancoff *et al.*, Appl Phys Lett **88**, 112507 (2005).
[6] J. C. Slonczewski, J Magn Magn Mater **159**, L1 (1996).
[7] L. Berger, Phys Rev B **54**, 9353 (1996).
[8] D. V. Berkov and N. L. Gorn, cond-mat/0601099 (2006).
[9] W. H. Rippard *et al.*, Phys Rev Lett **95**, 067203 (2005).
[10] W. H. Rippard *et al.*, Phys Rev B **70**, 100406(R) (2004).
[11] G. Gioia and R. D. James, Proc R Soc Lond A **453**, 213 (1997).
[12] M. A. Hoefer, Ph.D. thesis, University of Colorado, Boulder (2006), http://amath.colorado.edu/activities/thesis/PhD.html.
[13] W. E and X.-P. Wang, SIAM J Numer Anal **38**, 1647 (2000).
[14] M. R. Pufall, W. H. Rippard, and T. J. Silva, Appl Phys Lett **83**, 323 (2003).